JOURNAL OF VIROLOGY, June 2008, p. 5750–5760 Vol. 82, No. 12
0022-538X/08/$08.00+0 doi:10.1128/JVI.02673-07

Sindbis Virus Conformational Changes Induced by a Neutralizing Anti-E1 Monoclonal Antibody▽

Raquel Hernandez,[1]* Angel Paredes,[2] and Dennis T. Brown[1]

Department of Molecular and Structural Biochemistry, North Carolina State University, Raleigh, North Carolina 27608,[1] and University of Texas Health Sciences Center, Houston, Texas 77030[2]

Received 17 December 2007/Accepted 6 April 2008

A rare Sindbis virus anti-E1 neutralizing monoclonal antibody, Sin-33, was investigated to determine the mechanism of in vitro neutralization. A cryoelectron microscopic reconstruction of Sindbis virus (SVHR) neutralized with FAb from Sin-33 (FAb-33) revealed conformational changes on the surface of the virion at a resolution of 24 Å. FAb-33 was found to bind E1 in less than 1:1 molar ratios, as shown by the absence of FAb density in the reconstruction and stoichiometric measurements using radiolabeled FAb-33, which determined that about 60 molecules of FAb-33 bound to the 240 possible sites in a single virus particle. FAb-33-neutralized virus particles became sensitive to digestion by endoproteinase Glu-C, providing further evidence of antibody-induced structural changes within the virus particle. The treatment of FAb-33-neutralized or Sin-33-neutralized SVHR with low pH did not induce the conformational rearrangements required for virus membrane-cell membrane fusion. Exposure to low pH, however, increased the amount of Sin-33 or FAb-33 that bound to the virus particles, indicating the exposure of additional epitopes. The neutralization of SVHR infection by FAb-33 or Sin-33 did not prevent the association of virus with host cells. These data are in agreement with the results of previous studies that demonstrated that specific antibodies can inactivate the infectious state of a metastable virus in vitro by the induction of conformational changes to produce an inactive structure. A model is proposed which postulates that the induction of conformational changes in the infectious state of a metastable enveloped virus may be a general mechanism of antibody inactivation of virus infectivity.

Many protein structural intermediates are required for the assembly of infectious virus particles, and after virus binding to the host cell receptor, many structural changes occur during the process of infection. The immune system responds to the multiple conformations presented by a virus during an infection with a vast array of neutralizing antibodies (Abs). One mechanism of virus neutralization which is not well described is proposed to involve Ab induction of conformations which disrupt infection. Examples of neutralizing Ab-inhibited or Ab-induced conformational changes exist for an array of viruses. The best-described virus system that illustrates the importance of these transient protein states during infection is that of the influenza virus (family *Orthoviridae*), which undergoes a complex set of conformational changes induced by low pH to deliver the virus genome into the host cell by virus-cell fusion (12, 59). For the influenza system, the best understood mechanism of Ab neutralization is by blocking virus attachment to the host cell. However, Abs that neutralize fusion activity have been identified, suggesting interference with the conformational changes involved in membrane fusion (12, 13, 21), thus blocking intermediate structures required for infection. It has also been proposed that immune neutralization of human immunodeficiency virus (HIV) (family *Retroviridae*) by monoclonal antibodies (MAbs) involves a similar type of mechanism to disrupt infectivity involving Ab interference with structural rearrangements that are required for fusion (5, 9). Additionally, evidence for "conformational camouflage" has been presented to explain how HIV resists Ab neutralization through conformational masking of the receptor-binding sites on the virus requiring induced conformations to bind the receptors (27). It has previously been demonstrated that antibody neutralization of HIV follows single-hit kinetics, implicating an alternative mechanism to that of binding occlusion or steric hindrances (32). Certain Abs against respiratory syncytial virus (family *Paramyxoviridae*) and rabies virus (family *Rhabdoviridae*) have also previously been shown to neutralize virus infection by inducing conformational changes in virus structure (8, 22, 23). Virus neutralization through Ab-induced conformational changes has previously been proposed for nonenveloped viruses, such as rotavirus (family *Reoviridae*) and poliovirus (family *Picornaviridae*) (41, 54, 62). Studies using poliovirus demonstrated that virus neutralization could occur with one or two Ab molecules per virion (61). While Ab-mediated binding occlusion or steric interference may be the best understood mechanism of virus neutralization, mounting evidence suggests that virus neutralization mechanisms can disrupt infection by interfering with the development of conformations of the virus particle required for any phase of the infection pathway (8, 45, 54).

The investigation of neutralized virus structures has been studied through the use of crystallography and cryoelectron microscopy (cryo-EM) by analysis of native virus proteins or virus particles complexed with neutralizing Ab or FAb. For the alphaviruses (family *Togaviridae*), mechanisms of virus neutralization have previously been evaluated using structural methods. One type of neutralizing structure was described for Sindbis virus (SVHR) and Ross River virus by using two different cognate anti-E2 neutralizing FAbs (55). The structures solved

* Corresponding author. Mailing address: Department of Molecular and Structural Biochemistry, North Carolina State University, Campus Box 7622, Raleigh, NC 27695-7622. Phone: (919) 515-5765. Fax: (919) 515-2047. E-mail: raquel_hernandez@ncsu.edu.

▽ Published ahead of print on 16 April 2008.

for these virus-antibody complexes suggested a mechanism of neutralization and determined the location of the E2 epitopes on the surfaces of virions (55). In that study, Smith et al. suggested that virus neutralization by the anti-E2 MAbs tested was the result of Ab occlusion of the region of E2 that engages the cellular receptor. This type of occlusion mechanism has been widely proposed for the neutralization of many diverse viruses (25, 45, 47, 54). For Sindbis virus, most neutralizing Abs are found to react against the E2 glycoprotein, while neutralizing Abs directed against E1 are rare (57). This bias of the immune response to infection by SVHR probably reflects the highly metastable nature of the E1 protein, which may not retain the native state when released from the E1-E2 heterodimer during the immune response (34–36). One MAb isolated against SVHR E1, Sin-33, was shown to be an effective neutralizing Ab (53). In the present study, structural and biochemical evidence is presented which invokes an alternative mechanism to that of epitope occlusion of SVHR neutralized by Sin-33 or FAb-33. This model posits that an alternative mechanism of in vitro virus neutralization involves Ab-induced conformational changes of the virion to produce a noninfectious state. FAb-33-neutralized SVHR was shown by cryo-EM to have structural changes in the virus surface, with no apparent effect on the underlying core structure at 24-Å resolution. The altered structure of the neutralized virus was induced by FAb-33 binding in an epitope-to-paratope stoichiometry of less than 1:1, as shown by a lack of FAb density in the three-dimensional reconstructed density map. This reconstruction was corroborated by biochemical evidence demonstrating FAb binding at about 30% occupancy. The conformational changes produced by Sin-33 and FAb-33 were also shown to interfere with the structural rearrangements induced by low pH, thus inhibiting cell-cell fusion, but the changes did not interfere with virus association to the cell. This neutralized SVHR structure is the first reconstruction of an Ab-induced noninfectious conformational state of an enveloped virus particle.

MATERIALS AND METHODS

Cryo-EM and image reconstructions of Sin-33 FAb-treated SVHR. Purified SVHR was complexed with FAb from MAb 33, referred to here as Sin-33. FAb molecules were used to optimize data collection and to minimize any possible steric interference from the Fc portion of the immunoglobulin G (IgG). Sin-33 was originally isolated using SVHR strain AR339 (56, 57), but is highly neutralizing to SVHR (this study), which differs from the AR339 E1 sequence at amino acid positions 72 (A→V), 157 (K→N), 237 (S→A), and 399 (Q→L). Escape mutants of Sin-33 were found to carry changes at amino acid position 132 (57), which is proximal to the glycosylation site at N 139 and has previously been shown to be exposed to cleavage by furin (37).

Vitrified specimen was prepared by applying either FAb-treated or untreated SVHR onto glow-discharged holey carbon EM grids (400 mesh) prepared by previously published methods (40). The grids were then blotted with filter paper and quickly plunged into a liquid ethane slurry maintained by liquid nitrogen and then stored in liquid nitrogen prior to use. Cryo-EM was performed using both a JEOL 4000 cryoelectron microscope (magnification of ×50,000), operating at 400 keV (the 400-keV machine), and a JEOL1200 cryoelectron microscope (magnification of ×30,000), operating at 100 keV (the 100-keV machine). The higher-voltage microscope was used for resolution, and the lower-voltage microscope was used for contrast. The specimen was maintained at a constant −169°C, and images of virus were recorded on Kodak SO-163 EM film which was developed for 12 min at 20°C. Focal pair images, close and far from focus, were recorded with different defocuses used for the first close-to-focus image, and the same defocus difference was used between focal pairs.

The JEOL 1200 microscope was used to record images for both untreated control virus and Sin-33 FAb-treated virus. The images of untreated control viruses collected with this microscope were processed as described below and resulted in a three-dimensional reconstruction. Because this structure was similar to previously published alphavirus structures, we used it to make comparisons with the treated virus. The FAb-33-treated virus was processed first by using data from the 100-keV microscope. These data were refined and produced a low-resolution structure that was then used to refine data obtained from the 400-keV machine. The final comparison was made using the higher-resolution 400-keV structure. The data for the untreated control were scanned with a Zeiss scanner and resulted in images of a pixel size of 4.3 Å/pixel. Micrographs of FAb-33-treated virus from the JEOL 4000 and the JEOL 1200 microscopes were digitized on a Nikon 8000 scanner, resulting in a final pixel size of 3.2 Å/pixel for data from the 400-keV machine and 4.3 Å/pixel for data from the 100-keV machine. The processing of untreated virus taken with the JEOL 1200 and scanned with the Nikon 8000 shows the same results as described above and indicates that the scanner was not an influence on the data (data not shown). The processing of the lower-voltage images of treated virus gave us, first, two independent reconstructions from two different microscopes and, second, a preliminary model. This model was scaled and used to refine the higher-resolution images from the JEOL 4000. In all, there were seven close-to-focus micrographs recorded with the JEOL 4000 of FAb-treated SVHR, with the defocus value used in the final reconstruction ranging from −0.9 to 3.0 μm. The seven micrographs produced 874 virus images of FAb-treated virus. All FAb images were processed and reconstructed using two independent methods, (i) hierarchical wavelet transformation and projection matching according to previously published procedures and (ii) EMAN, a single-particle analysis and reconstruction program, where icosahedral symmetry was imposed in the final reconstruction (29, 48, 49). The wavelet transformation program works as a denoising method that enhances contrast by converting the input image into an approximation component (49). Orientations of these processed virus images were then determined by matching them against projections of known orientations from a previously published model (15, 39). These orientations were then refined against each other using the cross-common lines method to produce the final three-dimensional map.

In the EMAN reconstruction, both untreated control virus and FAb-treated virus images were filtered to their first zero and then processed by the software to select the best three-, five-, and twofold virus images. These images were then averaged into three-, five-, and twofold class averages, which were then averaged into an initial three-dimensional map by first merging them and then applying icosahedral symmetry to them. The resulting model was a very-low-resolution preliminary map without much detail. This map was used as an initial model for refinement of the data, which was accomplished by first reprojecting it into a set of projections of known orientations. The raw data was then refined against these projections to produce a set of class averages composed of virus images aligned with each other and summed together to reduce noise. These class averages were then assembled into a new three-dimensional map which was then reprojected into a new set of projections that was used to refine the data again in an iterative process. After nine iterations, a final low-resolution map was evaluated. Images from the 400-keV microscope were processed in exactly the same manner as that described above, with the exception that the map produced from the 100-keV microscope was subsequently scaled to match and refine the data from the 400-keV machine. We compared the results of this methodology to previously published structures of SVHR and to the structure produced in this study of untreated control using the same methodology as that for treated virus. The maps were rendered and displayed using UCSF chimera (42).

Virus growth, purification, and titration. BHK cell culture conditions and SVHR infections were as described previously (16, 46). Virus was metabolically labeled using [^{35}S]methionine-cysteine (PerkinElmer, Wellesley, MA) as described previously (50) and purified and quantitated by scintillation spectrometry and bicinchoninic acid analysis (Pierce, Rockford, IL) following the manufacturer's procedures. SVHR was the virus strain chosen because of the very low (ca. 1) particle-to-PFU ratios this strain produces. Virus preparations were purified twice by using 15 to 35% or 20 to 35% potassium tartrate gradients prepared in 20 mM MOPS (morpholinepropanesulfonic acid), pH 7.4, 100 mM NaCl, pH 7.4 (51). Both purifications were performed using a Beckman SW28 rotor at 24,000 rpm for 12 h. The virus bands were collected and dialyzed twice against 20 mM MOPS, pH 7.4, 100 mM NaCl. After dialysis, virus was concentrated by burying the bag under Sephadex G-100 beads and sweating the bag until the desired concentration was achieved. SVHR virus titers and SVHR neutralization by Sin-33 and FAb-33 were determined by virus titration using a standard plaque assay (46), and virus neutralization was determined using the plaque reduction assay (52).

Sin-33 and FAb-33 purification and preparation of treated SVHR. MAb 33 (Sin-33), a generous gift from Alan Schmaljohn, U.S. Army Medical Research Institute of Infectious Diseases, has previously been described (52, 53). This MAb was shown to be specific for SVHR E1 and recognized an epitope on

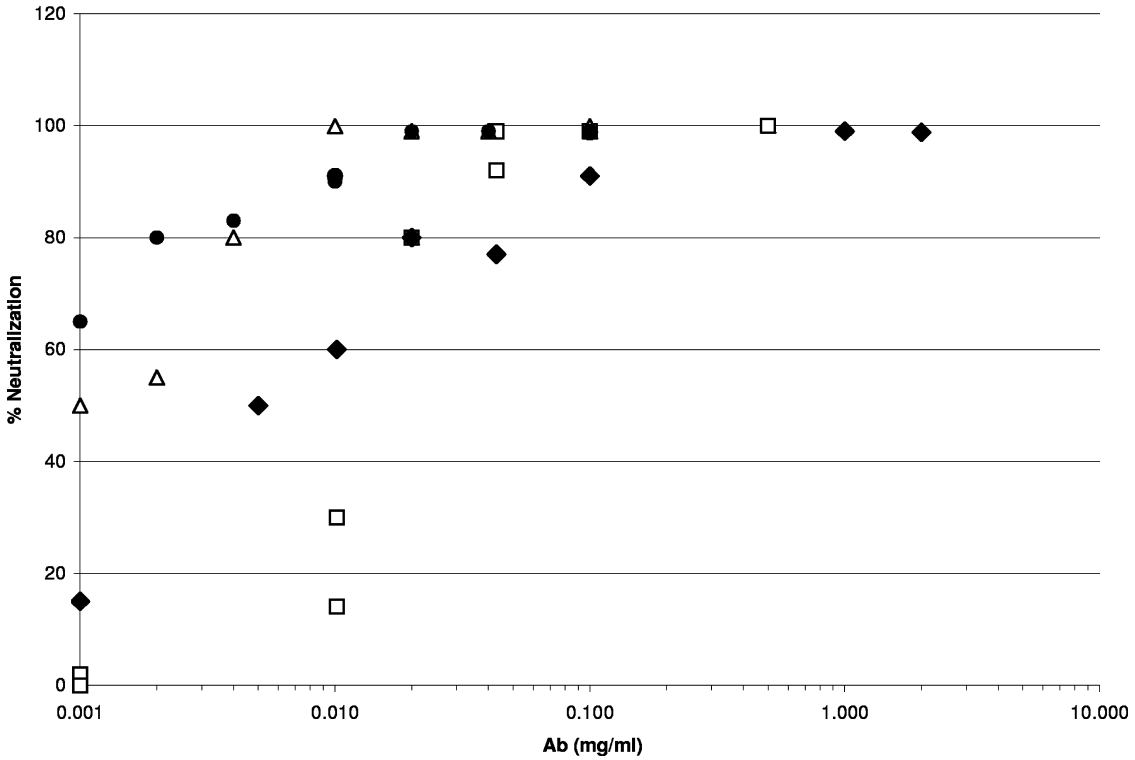

FIG. 1. Plaque reduction neutralization assays of SVHR treated with Sin-33 Ab (□) or FAb-33 (◆) for 15 min at 25°C or Sin-33 (●) or FAb-33 (△) treatment at 4°C overnight. Ab was added at the indicated concentrations, and incubations were performed as described in Materials and Methods. Neutralizing Ab concentrations of 90 to 100% (0.1 mg/ml) in an overnight treatment at 4°C were chosen for subsequent experiments.

nondenatured virus particles (53). This MAb was also the only anti-E1 MAb of this group that demonstrated virus-neutralizing activity and was found to be more effective in the ablation of plaques than the characterized anti E2 MAbs were (53). Sin-33 IgG was purified from lyophilized ascites by dissolving 40 mg of the Sin-33 containing material in 1 ml of phosphate buffer (20 mM NaH_2PO_4, 20 mM Na_2HPO_4, pH 7.0). IgG was purified using a HiTrap protein A affinity column (Amersham Biosciences, Piscataway, NJ) according to the manufacturer's instructions by using an Aktaprime fast-protein liquid chromatography instrument (Amersham Biosciences, Piscataway, NJ). FAb-33 was produced by digestion of Sin-33 MAb using 10 μg of papain (Roche Diagnostics, Alameda, CA) for each milligram of antibody at 37°C for 4 h by using standard conditions as follows and as detailed previously (43, 44). Briefly, protease stock (10 mg/ml in H_2O) was activated in 1 mM EDTA, 50 mM cysteine, 50 mM sodium phosphate, pH 7.0, buffer at 37°C for 10 min prior to the digestion reaction at a final concentration of 1 mg/ml. Purified IgG in digestion buffer (100 mM CH_3COONa, pH 5.5, 50 mM cysteine, and 1 mM EDTA) was digested with papain at a wt/wt ratio of 1:200 papain to IgG, at 37°C for 3 h, and the reaction was quenched by using 75 mM iodoacetamide at room temperature for 30 min. Digestion was monitored on 15% sodium dodecyl sulfate (SDS)-polyacrylamide gel electrophoresis gels, and FAb was identified after reduction with dithiothreitol as a peptide doublet running at about 25 kDa. FAb peptides were separated from any undigested IgG and Fc using the HiTrap protein A column and the method described above, except that the flowthrough fraction containing the FAb-33 was collected and concentrated using Centricon 10 devices (nominal molecular weight limit, 10 kDa; Millipore, Bedford, MA). The FAb-33 protein concentration was determined by using a bicinchoninic acid kit (Pierce, Rockford, IL).

Neutralization of SVHR by Sin-33 and FAb-33. To more accurately quantify the amount of Sin-33 and FAb-33 required to inactivate a constant number of SVHR particles, the particle-to-PFU ratios of purified virus were first determined as described in reference 19 and virus samples chosen for this study were in the range of 1 to 10 particles per PFU (average, <5 particles per PFU). For all virus samples, SVHR was purified, titers were determined, and SVHR was quantitated as described above. Virus neutralization determinations were performed with high concentrations of virus to better assess the Ab activity at the high virus concentrations used in all subsequent experiments. To determine the neutralization titers of purified Sin-33 or FAb-33 necessary to inactivate 10^{10} PFU of purified SVHR, Sin-33 or FAb-33 was added (in the concentrations specified in Results) and allowed to adsorb to the virus for 15 min at room temperature or at 4°C overnight in 100 μl of 20 mM MOPS, pH 7.4, 100 mM NaCl, pH 7.4 (39). Virus titration was as described above. For virus neutralization of samples for cryomicroscopic analysis, a fivefold molar excess of FAb/E1 was added to 6×10^{12} total PFU of twice-purified SVHR and allowed to bind at 4°C overnight as reported previously for FAb neutralization of SVHR (55) and rotavirus (41). This method was chosen over the 15-min room temperature incubation because it produced much less aggregation of the virus particles, and gave consistently higher virus neutralization titers.

Peptide mapping of FAb-treated radiolabeled SVHR. For peptide mapping of SVHR, 100 μl of [^{35}S]methionine-cysteine-labeled, twice-purified virus (200,000 counts per minute/ml, 12.5 μg of virus) was incubated with 2 μg FAb-33 overnight at 4°C as described above in a total reaction volume of 150 μl. FAb-33-bound labeled virus was digested with 125 μg/ml endoproteinase Glu-C (V-8) in 25 mM $(NH_4)_2CO_3$, pH 7.8, for 6 h at 37°C. Proteolysis was terminated by the addition of 1 mM phenylmethylsulfonyl fluoride (Sigma, St. Louis, MO) and the addition of polyacrylamide gel electrophoresis sample buffer (12.5 mM Tris-Cl, pH 6.8, 5% glycerol, 1% SDS, 0.01% bromophenol blue, and 1% β-mercaptoethanol) followed by heating to 100°C for 5 min. Peptides from the digests were separated on 10% Tricine gels as described previously (30).

FFWO with FAb-33-neutralized SVHR. Conditions for SVHR fusion from without (FFWO) have been described previously for BHK cells (10, 11). The level of FFWO for FAb-33-treated virus was determined by incubating twice-purified virus with FAb-33 as described above, with corresponding concentrations of FAb-33 to give more than 90% neutralization after an overnight incubation at 4°C (Fig. 1 shows virus-to-Ab ratios). BHK cells in 12-well plates were then exposed to 1,000 PFU/cell of the FAb-33-treated virus, followed by a 5-min incubation at 37°C with fusion medium (10, 11) and a return to pH 7.3. After 1 h, the cell monolayers were scored for the amount of fusion compared to the positive (with SVHR plus low-pH treatment) and negative (lacking SVHR with low-pH treatment) control wells. The percent fusion was determined relative to that of the untreated control, and the 100% fusion level was relative to the

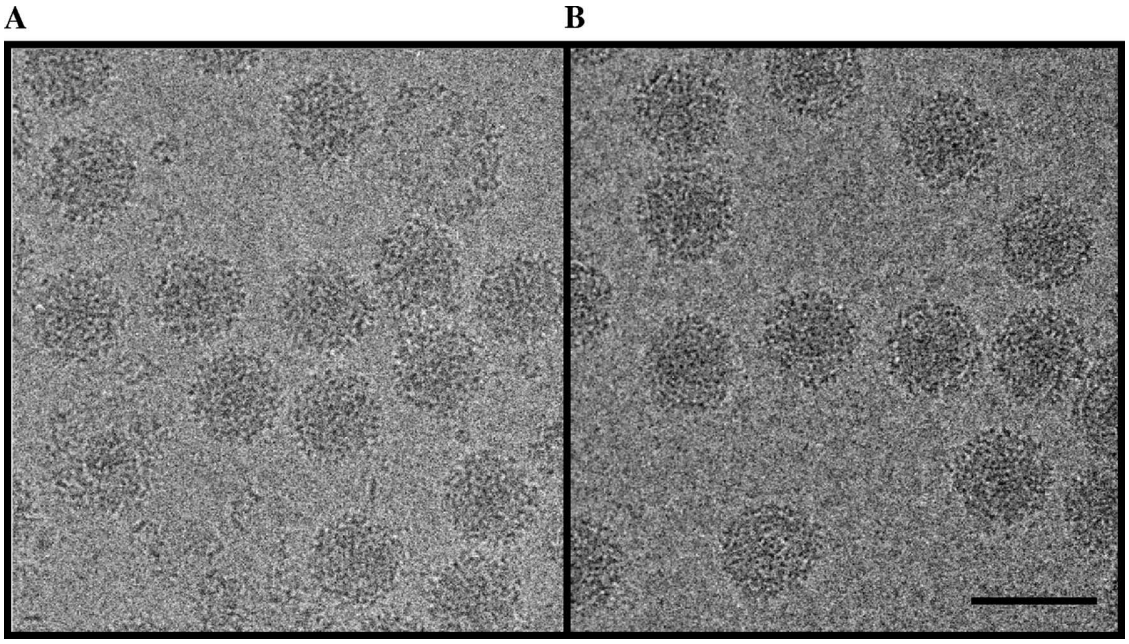

FIG. 2. Cryoelectron micrographs of (A) untreated Sindbis virus and (B) FAb-33-bound Sindbis virus treated at 4°C overnight with 0.1 mg/ml purified FAb-33. Scale bar, 1,000 Å.

controls treated at pH 7.4 (pH 7.4-treated) as previously reported in references 10, 11, and 31.

Iodination of Sin-33 and FAb-33 and virus binding assays. Iodination reactions were carried out using the IODO-GEN (Pierce, Rockford, IL) iodination reagent according to the manufacturer's standard protocol. For the low-pH experiments, a total of 500 μg of Sin-33 or FAb-33 was iodinated using 500 μCi/100 μg carrier-free ^{125}I (PerkinElmer, Boston, MA). After stopping the iodination reaction, Ab was washed away from unincorporated iodine with four washes of 2 ml phosphate-buffered saline (PBS)-D (phosphate-buffered saline [PBS] lacking Ca^{2+} and Mg^{2+} [20]) by using Centricon 50 spin dialysis devices (50-kDa molecular weight limit). Iodinated Ab was then added to purified SVHR (which was determined to have a particle-to-PFU ratio of 1) at a ratio of 0.1 μg/ml (Sin-33 or FAb-33)/10^{11} PFU/ml virus (more than 99% neutralization for both Abs) at 4°C overnight. To determine the effect of pH 5.3 treatment on virus bound Ab, ^{125}I-labeled Sin-33 or FAb-33-neutralized virus (as prepared above) was taken to pH 5.3 for 5 min and returned to pH 7.4 by titration with 1 M MOPS, pH 5.3, followed with 1 M Tris, pH 7.4, or treated only with 1 M Tris, pH 7.4. Unbound or released Ab was separated from virus-bound Ab by centrifugation through 17 ml of 15 to 35% K-tartrate gradients (see "Virus growth, purification, and titration" above). Peaks of virus bound with Ab were determined by scintillation spectrometry of gradient fractions. For stoichiometric determinations of FAb-33 binding to SVHR, 9 μg of FAb-33 was iodinated with 1 mCi of carrier-free ^{125}I by using the same IODO-GEN chemistry as that described above. After stopping the reaction, protein was purified away from unincorporated label by using Zeba desalt spin columns (0.5 ml; Pierce, Rockford, IL) according to the manufacturer's instructions using two consecutive columns. Virus-to-FAb ratios were maintained at the concentrations described above. Virus bound with FAb-33 was separated from unbound FAb-33 by using a 14 ml of 15 to 35% K-tartrate gradient centrifuged for 190 min in a Beckman Ti 40 rotor at 30,000 rpm. The gradients were collected as 10-drop fractions and counted using a 1480 Wallac Wizard 3 gamma counter (PerkinElmer, Shelton, CT). FAb-33-specific activity was determined, and the amount of protein bound/virus particle in the virus peak was determined.

Cell binding assay. Radiolabeled virus was prepared as described previously (2). BHK cells were prepared as described above to be about 90% confluent in a 24-well plate. Cells were chilled on ice for 15 min prior to the addition of virus (about 3,000 counts per min per well and about 1,000 PFU per cell) pretreated with a neutralizing concentration of Ab (1 μg Sin-33 or FAb-33 added to 10^{10} PFU of virus for 15 min or at 4°C overnight) or PBS buffer in 100 μl added to six wells. Attachment proceeded on ice for 1 h with rocking. After the attachment period, the inoculum was removed and the monolayers were washed three times with 500 μl PBS. The cell monolayers were harvested using lysis buffer (28). All fractions, inocula, washes, and cells were collected and counted by scintillation spectrometry.

Protein structure accession number. The data has been deposited in the EMBL-EBI Macromolecular Structure Database (www.ebi.uk/msd/index.html) in the EMDep data bank. The accession number is EMD-1437 for the map entry.

RESULTS

Sin-33 and FAb-33 SVHR-neutralizing titers. Previously, Schmaljohn et al. (53) determined that a 10^{-3} dilution of Sin-33 IgG from ascites fluid (~1 to 10 mg/ml ascitic fluid) neutralized 80% of 100 PFU of SVHR in the presence of 5% (wt/vol) guinea pig complement or produced 50% neutralization in the absence of complement (56). In the present study, purified SVHR at high virus concentrations (10^{10} total PFU) was titrated (in the absence of added complement) by incubation with increasing concentrations of purified Sin-33 or FAb-33 for 15 min at room temperature or at 4°C overnight. The virus samples used for these titrations were determined (as described previously by Hernandez et al. [19]) to have an average of five particles per PFU (data not presented). While plaque reduction neutralization titers are generally performed with a low number of virus particles to minimize titration errors (26, 58), the neutralization characteristics of Sin-33 and FAb-33 on highly concentrated virus were established, as these concentrations would be required for the following structural and biochemical analyses. To determine whether FAb-33 significantly differed from the intact Sin-33 Ab in affinity or avidity due to factors such as a change in valence, virus neutralization was conducted with virus at concentrations of 10^{10} PFU/100 μl. As shown in Fig. 1, the neutralization curves of Sin-33 IgG and that of FAb-33 converge at a concentration of ~20 μg/ml, which was found to neutralize 80% of the input virus

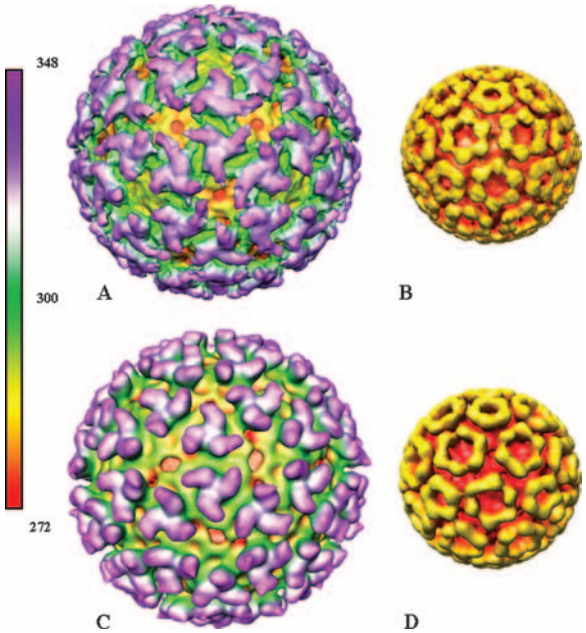

FIG. 3. Cryo-EM structures of FAb-33-treated SVHR (A) and untreated SVHR (C) viewed along the icosahedral threefold axis at 24-Å resolution. Shown in panels B and D are the extracted capsid structures from the FAb-33 and nontreated SVHR structures, respectively, which can also be viewed along the icosahedral threefold axis. The reconstructions are color coded according to the radial distance (Å) as indicated in the key.

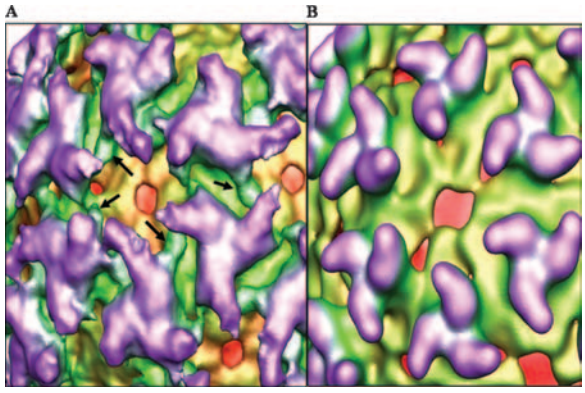

FIG. 4. Enlarged surface structure of FAb-33-treated SVHR (A) and control SVHR (B). (A) An enlarged and skewed view of the strict twofold axis of the FAb-33-treated virus to better display the distortion of the trimer trunk. Note the tapering and deformation of each of the lobes of the trilobed E2 spikes at the strict threefold and around the fivefold and twofold axes. The region under each trimer toward the outer shell orifice is also altered and appears to have extra density that extends away from the trunk of the trimer and is disorganized (arrows). E2 within the heterotrimeric spikes acquires a conformation which along with E1 reduces density within the fenestrations found at the threefold and fivefold axes. (B) An area on the nontreated control virus equivalent to that presented in panel A is shown for comparison. Color cueing was applied to the radii pertaining to the skirt region (yellow/green, yellow having a slightly shorter radius), the trimer trunk rising from the skirt region (green), and the trimer lobes (purple).

during an incubation period of 15 min at room temperature. These concentrations of Sin-33 and FAb-33 represent a 3.3-fold and 10-fold, respectively, molar excess of Ab to E1. The approximately threefold difference demonstrates that FAb-33 paratopes closely parallel those of Sin-33 IgG in their abilities to neutralize the majority of added virus and thereby demonstrate that the effect of FAb-33 on virus is not significantly different than that of the intact Ab. Additionally, the high levels of neutralization achieved by IgG and FAb within 15 min at room temperature and the ability to dilute out the Ab and retain these levels of neutralization suggest a moderate affinity and avidity for FAb and IgG, respectively. The levels of virus neutralization with Sin-33 or FAb-33 were found to increase as the time of incubation to Ab was extended in an overnight incubation at 4°C, and it was determined that a fivefold molar excess of FAb-33 was sufficient to neutralize more than 90% of 10^{10} PFU of SVHR when incubations were carried out at 4°C overnight. This method was adopted for the FAb-virus treatments used to prepare the virus used in the reconstruction for the reason stated above in Materials and Methods.

Image reconstructions of FAb-33-treated SVHR. Comparisons made between structures of FAb-treated virus produced by wavelet transformation and EMAN reveal that both methodologies produce very similar results (comparisons not shown). The wavelet transformation procedure involves using a preexisting Sindbis model to refine the data; therefore, to avoid questions of model bias, we only show and discuss the EMAN reconstructions where model bias is prevented by processing the data without influence from any previously derived model.

The three-dimensional reconstruction of SVHR particles treated with Sin-33 FAb under conditions which produced more than 90% neutralization or of control virus treated under the same conditions, in the absence of FAb, frozen in vitreous ice (Fig. 2), is shown as viewed down the strict threefold axis at 24-Å resolution (based on a Fourier ring correlation of 0.5) in Fig. 3 and 4. To better compare the three-dimensional structures, color cueing was applied to the radii pertaining to the skirt region, the trimer trunk rising from the skirt region, and the trimer lobes. The white region in the center of the trimer is an artifact of the lighting produced within the rendering software. In Fig. 3, panels A and C present the three-dimensional reconstructions of the FAb-treated and control virus, respectively, while panels B and D present their respective nucleocapsid structures. We were able to independently evaluate the accuracy of the FAb-treated reconstruction by extracting the nucleocapsid structure from the full volume and comparing it to the nucleocapsid from the untreated virus. As shown in Fig. 3B and D, the nucleocapsid structures appear very similar at 24 Å (jagged edge effect present in the FAb-treated nucleocapsid is an artifact of the software used to extract the nucleocapsid from the intact volume). In fact the nucleocapsid structure of the FAb-treated virus appeared to be slightly better than the untreated virus with respect to previously published nucleocapsid structures (38). The quality of the FAb-treated nucleocapsid gave us confidence that the structure of the intact virus was correct.

While significant conformational changes were visible in the FAb-treated SVHR particles (Fig. 3A), no density corresponding to the FAb-33 molecules was detected, as was reported for neutralizing Abs against E2 (55). The untreated control virus

TABLE 1. SVHR binding assay

Parameter	Value for SVHR incubated with[a]:				Value for SVHR control
	FAb ON	FAb for 15 min[b]	Sin-33 ON	Sin-33 for 15 min[b]	
Inoculum	53.98 ± 3.57	51.52 ± 3.19	56.39 ± 5.83	58.22 ± 2.44	56.32 ± 5.34
Washes	6.21 ± 0.82	7.24 ± 0.34	7.54 ± 1.24	6.81 ± 0.64	6.03 ± 0.69
Cells plus virus	39.80 ± 2.07	41.24 ± 2.07	36.08 ± 3.75	37.97 ± 1.26	37.65 ± 2.17

[a] ON, overnight 4°C. The ratio of cells plus virus fraction-to-virus control was 1.05 for SVHR incubated with FAb ON, 1.09 for SVHR incubated with FAb for 15 min, 0.96 for SVHR incubated with Sin-33 ON, and 1.01 for SVHR incubated with Sin-33 for 15 min.
[b] The 15-min incubations were at room temperature.

(Fig. 3C) showed no structural reorganization of the virus particles in the regions of the virion which are predicted to be occupied by E1 or E2 (63, 65) and the structure appeared as was previously described for SVHR (39). Structural alterations involving both E1 and E2 glycoproteins at each of the symmetry axes of the FAb-33-treated virus surface were visible reference to the untreated control (Fig. 3, compare panels A and C). As seen in Fig. 4A, which shows an enlarged and skewed view of the strict twofold axis of the virus, the neutralized virus exhibits a tapering and deformation of each of the lobes of the trilobed E2 spikes at the strict threefold axis and around the fivefold and twofold axes. In addition to the deformed lobes, the structure under each trimer is also altered (Fig. 4A and B). The regions beneath the trimers each appear to have extra density that extends away from the trunk of the trimer toward the skirt region and is disorganized. The regions of extra density were not of sufficient mass to represent density from a FAb molecule. Most notably in the FAb-33-treated virus seen in Fig. 4A, the predicted location of E1 within the heterotrimeric spikes acquires a conformation which reduces density within the fenestrations found at the three- and fivefold axes. Because of the lack of FAb-33 density, these results suggest that with respect to icosahedral reconstruction methods, the FAb may bind to the virus in undetectable quantities. FAb-33 molecules bound at levels much less than 50% occupancy would in fact be averaged out as noise. For any density to be represented in an icosahedral reconstruction, enough of that density must be present on the virus so that when icosahedral symmetry is imposed on the data during the image processing, the density is reinforced. Since alphaviruses have $T=4$ symmetry, we expect 240 copies of any density on the virus surface, including epitopes bound with Ab. If too few FAbs bind to their respective epitopes and particularly if their placement is random, FAbs as densities would be either averaged out in the final reconstruction or appear as random noise around their epitope on the virus. This lack of any density that could be considered FAb in the reconstruction combined with the observation that the conformational changes observed were seen throughout the virus structure suggests that the conformational shifts seen for both E1 and E2 may have been induced by the binding of a small number of FAb molecules. While it would be expected that 240 E1 epitopes would bind FAb, E1 epitopes could be lost if the initial conformational shifts were to induce cascading changes throughout the virus occluding the remaining anti-E1 epitopes. This hypothesis would predict that no FAb density would be detected, even under conditions in which the avidity of the FAb was high. The data generated by these reconstructions suggest that the structural rearrangements affected by FAb-33 result in neutralization of the virus by altering the conformation of E2 required for binding of the virus to the cellular receptor and/or by shunting E1 into a conformational intermediate incapable of proceeding through the remaining conformational changes required for infection (40). The possibilities that less than the 1:1 stoichiometric ratio of E1 epitopes was bound by FAb-33 and that induced conformational changes may affect virus binding to the host cell were tested.

Cell binding of Sin-33-neutralized and FAb-33-neutralized SVHR. To determine whether FAb-33-neutralized virus particles retain the ability to bind to cells, treated and untreated radiolabeled virus was tested for cell binding as described in Materials and Methods. The results of this experiment are shown in Table 1 and show that SVHR treated with FAb overnight (40%) or for 15 min (41%) compared to SVHR treated with Sin-33 overnight (36%) or for 15 min (38%) did not significantly affect the amount of labeled virus bound to cells compared to the SVHR control (38%). Because the virus cell receptor is not known, it is not possible to specifically differentiate between binding and adherence. Given that the particle-to-PFU ratio for this virus is ~3 to 5, ca. 38% of label associated with the cells should correspond to binding/adherence. These data demonstrate that there was no difference in the amount of Sin-33-treated or FAb-33-treated virus bound to cells relative to amount of untreated control virus. These data suggest that Sin-33 and FAb-33 neutralization of virus did not affect the association of virus particles with cell monolayers. This assay, however, could not specifically differentiate between specific virus binding to cell receptors or nonspecific virus adherence, which is known to occur with SVHR particles displaying altered conformations (17, 40). It was of interest, however, to determine whether the conformational state displayed by the FAb-33-neutralized virus seen in the reconstruction was in a locked structure or whether these particles could be induced to undergo further changes. To test this possibility, neutralized particles were assayed for their abilities to induce FFWO, a reaction which requires structural rearrangements of both E1 and E2 glycoproteins (40).

FAb-33-neutralized, SVHR-mediated FFWO. Of the MAbs produced by Schmaljohn et al., Sin-33 was found to be the best inhibitor of pH-dependent fusion from within (FFWI) (52, 53). To determine the ability of FAb-33 to reproduce this result and also to test the possibility that the neutralized virus conformation might retain the capacity to undergo further structural changes, FAb-33-treated virus was tested by FFWO of BHK cells. Twice-purified SVHR with a particle-to-PFU ratio of ~1 was treated with increasing concentrations of FAb-33 and the

TABLE 2. Inhibition of FFWO by FAb-33 treated SVHR[a]

FAb (μg/100 μl)	Relative fusion (%)[b]	% Virus neutralization	Fusion (%) of control SVHR
1,000	0	100	100
100	10	100	100
10	10	90	100
2	60	80	100
1	100	60	100
0.1	100	18	100

[a] PFU/100 μl of twice-purified virus at particle/PFU ratio of ca. 1. All virus amounts were 10^{10} PFU.
[b] Fusion level relative to that of untreated control virus.

relative levels of fusion (evaluated as in reference 11) were determined and are presented in Table 2. Our results reproduced the previously published observations which identified Sin-33 as a strong inhibitor of FFWI and extended these observations to include the inhibition of virus-mediated FFWO by FAb-33-treated SVHR. While this type of study is subjective, these data suggest that increasing levels of fusion correspond with decreasing concentrations of FAb-33 and roughly correlate with virus neutralization. The direct effects of low pH on FAb-33 interactions with the virus are not known. However, these observations suggest that the FAb-33-induced conformation holds the virus particles in a structure which does not respond to low-pH-mediated triggers to produce a structure which adopts the fusion competent state (40). To test this possibility, the effect of low pH on the ability of Ab or FAb to remain bound to virus was tested directly using ^{125}I-labeled Sin-33 or FAb-33.

Effect of low-pH treatment on Sin-33 or FAb-33 bound to SVHR. The observation that the neutralization of SVHR by FAb-33-inhibited FFWO of BHK cells suggested that the neutralized virus may have adopted a dead-end, noninfectious structure incapable of additional conformational change. A second possibility was that the neutralized virus could be induced into alternate conformations by low-pH treatment, but did not achieve the structure required to drive the fusion reaction. It was also of interest to determine whether the low-pH treatment disrupted the binding of the Ab to the neutralized virus. To evaluate the effect of low-pH treatment on the ability of Sin-33 and FAb-33 to remain complexed with virus, ^{125}I-labeled Ab was incubated with 10^{10} total PFU of purified SVHR using neutralizing concentrations as described above. SVHR was incubated with ^{125}I-labeled Sin-33 or ^{125} I-labeled FAb-33, and the virus antibody complex was then exposed to a low pH or retained at a neutral pH, as described in Materials and Methods, prior to purification from unbound Ab by isopycnic centrifugation. As presented in Fig. 5A, during isopycnic centrifugation, ^{125}I-labeled Sin-33 complexed SVHR maintained at pH 7.4 banded in a narrow peak displaying virus density ($\rho = 1.17$ g/ml) (18), while the virus sample treated at pH 5.3 and returned to pH 7.4 displayed more virus-associated labeled Sin-33 in the virus fraction. The pH 5.3-treated sample displayed a large trailing shoulder of ^{125} I-labeled Sin-33 not seen in the pH 7.4 control, which represents a total of 58% more bound Ab in the low-pH-treated sample. This experiment was repeated with ^{125}I-labeled FAb-33 and is shown in Fig. 5B. Labeled FAb-33 in the low-pH-treated sample contained 68% more virus associated label than did the pH 7.4 control. These results suggest that pH 5.3 treatment of neutralized SVHR, followed by a return to neutral pH induces additional conformational changes within the virus structure (see reference 40). During the process of low-pH treatment, these newly exposed sites may have come into contact with labeled antibody allowing more Ab binding for both the IgG and FAb virus samples. This alternate conformation(s), however, while not achieving the fusion-inducing conformation may allow the virus to adopt a structure which exposes previously occluded E1 Sin-33 epitopes. The trailing shoulder of labeled complex in the low-pH-treated, neutralized virus sample also suggests that additional Ab bound to the virus particles is retarding sedimentation or altering the density of the complex. These results suggest that not all E1 epitopes are complexed with Ab and that upon low-pH treatment, additional sites become exposed to FAb, as was seen with the Sin-33 Ab. To determine the number of FAb molecules bound to SVHR under neutralizing conditions, the specific activity of the ^{125}I-labeled FAb-33 sample was determined and bound to two separate virus samples and, because the number of particles of virus was known, it was determined that between 60 ± 12 FAb molecules were bound per virus particle at pH 7.4. These data support the virus reconstructions presented in Fig. 3 and 4, which do not display FAb density, since this number of FAb molecules represents at most about 30% occupancy and would be averaged out.

Peptide mapping analysis of Sin-33 FAb-treated SVHR. To further demonstrate that significant structural rearrangement of the SVHR particles occurred upon virus treatment with Sin-33 FAb at low-epitope occupancy, [^{35}S]methionine-cysteine-labeled purified viruses, treated with or in the absence of FAb-33, were digested with V-8 protease. SVHR has been shown to be inherently resistant to digestion by proteases (11); however, high concentrations of proteases in conjunction with various treatments, such as heat, low pH, and dithiothreitol, have been used to digest the membrane glycoproteins (3, 11). Previous studies have shown that SVHR is resistant to proteolytic cleavage, with E1 displaying a higher sensitivity toward digestion than E2 does (3). SVHR was treated with a concentration of FAb-33 equivalent to that used to produce the virus samples for cryomicroscopy at 4°C overnight. The results of these experiments are shown in Fig. 6. Virus proteolysis required 6 h of incubation at 37°C using 125 μg/ml V-8 to detect the production of digestion products for the FAb-33-neutralized virus. Shown in Fig. 6 is [^{35}S]SVHR after treatments with V-8 and FAb. In Fig. 6, lane 1, is untreated [^{35}S]SVHR; in lane 2, virus associated with FAb is shown; in lane 3, [^{35}S]SVHR without FAb-33 treatment treated with V-8 is shown; and in lane 4, [^{35}S] SVHR plus FAb treated with V-8 is shown. SVHR treated with FAb-33 (Fig. 6, lane 4) was found to be more sensitive to V-8 digestion than was the untreated virus, and it rendered the virus into a conformation which displayed increased V-8 digestion. Previous work has shown that the treatment of SVHR to a pH level of 5.2 predisposes the virus to become more sensitive to trypsin or V-8 digestion (3, 11). The identity of the peptide fragments generated upon V-8 digestion could not be confirmed by this method since both E1 and E2 glycoproteins produce peptides of sizes similar to those of the four major products seen after digestion of the FAb-treated virus.

DISCUSSION

Antibody-mediated virus neutralization through the induction of conformational changes has previously been demon-

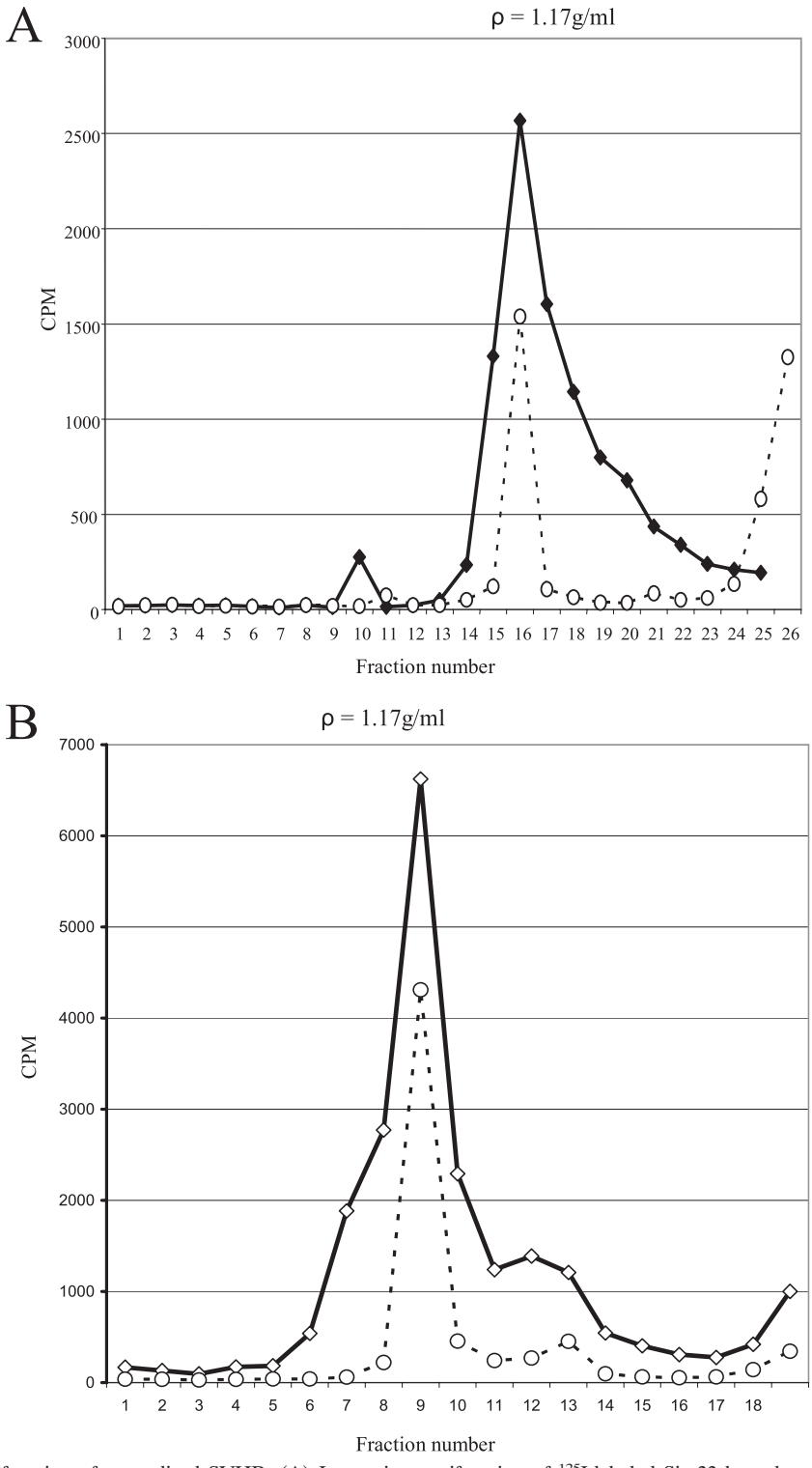

FIG. 5. Isopycnic centrifugation of neutralized SVHR. (A) Isopycnic centrifugation of ^{125}I-labeled Sin-33 bound to SVHR at pH 7.4 (○) or a duplicate sample after treatment at pH 5.3 and a return to pH 7.4 (◆). (B) Isopycnic centrifugation of ^{125}I-labeled FAb-33 bound to SVHR at pH 7.0 (○) or after treatment at pH 5.3 and a return to pH 7.4 (◇). Density of the radioactivity peak was 1.17 g/ml, which corresponds to the density of SVHR.

strated for nonenveloped and enveloped viruses. Specific examples of this type of mechanism are exemplified by studies using rabies virus and Venezuelan equine encephalomyelitis virus, which is also an *Alphavirus*. Virus neutralization of rabies virus by one specific MAb was proposed to be mediated through the binding of a few Ab molecules per virion, producing conformational changes which were propagated throughout the particle in a neutralization cascade termed

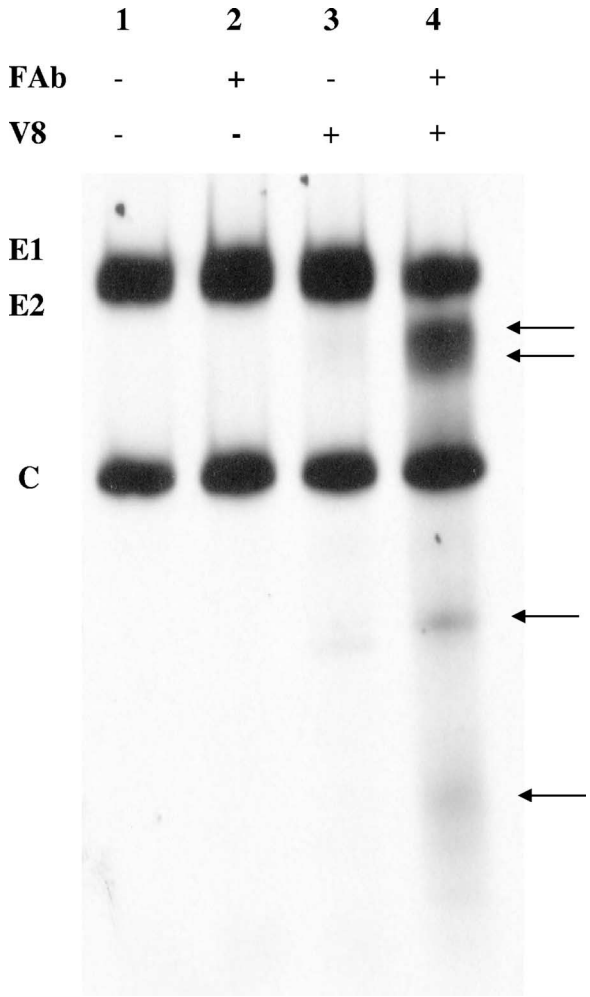

FIG. 6. Endoproteinase digestion map of FAb-33-treated SVHR. Shown is a 10% Tricine, polyacrylamide gel of FAb-33-treated or untreated [^{35}S]methionine-cysteine-labeled SVHR digested or undigested with endoproteinase Glu-C (V8). Lane 1, control SVHR untreated with FAb-33 or V8 (E1 and E2 comigrate under these conditions); lane 2, FAb-33-treated SVHR; lane 3, V8-treated SVHR. Note that SVHR is not sensitive to digestion under these conditions. Lane 4, FAb-33-treated, V8 endoproteinase-digested SVHR displaying four major digestion products (arrows). Capsid protein remains undigested in lanes 3 and 4 demonstrating that the virus particles remained intact during the digestion period. −, absence of; +, presence of.

the "domino effect" (22, 45). In that system, MAb-induced conformational changes induced by ≤20 molecules bound to G proteins (about 600 trimeric spikes per virion) were proposed to spread to neighboring G proteins, resulting in the loss of the receptor binding conformation of the remaining proteins and neutralization of the virion (23). Previous virus neutralization models proposed for Venezuelan equine encephalomyelitis virus suggested that virus glycoprotein conformations could be altered to stabilize virus-cell receptor interactions disrupting infection or by inducing the formation of noninfectious immune complexes which were still able to attach to cells (47). While suggested for enveloped viruses, this mechanism of virus neutralization did not have direct structural evidence.

The present study supports the concept of Ab-mediated conformational changes as a general mechanism of virus neutralization and a specific method for SVHR which may apply to other alphaviruses. Stoichiometric determinations of the number of FAb-33 molecules associated per virus particle were calculated to be about 60 FAb molecules. The observation that few molecules of antibody are required to neutralize a virus particle is consistent with the lack of FAb density seen in the reconstructions of FAb-treated SVHR which displayed epitope binding stoichiometry of less than 1:1. Our results demonstrate that under neutralizing conditions, FAb-33 molecules bound to SVHR at about 30% occupancy and induced structural reorganizations which altered the virus surface, resulting in a noninfectious particle. The resultant conformational changes of FAb-33-neutralized SVHR, however, did not block attachment of virus to cells. The inability to detect FAb density in the cryo-EM reconstruction is due to the limitations of the techniques used, which can only resolve structure when 60-fold icosahedral symmetry is imposed. While asymmetric reconstructions of bacteriophages P22 (7) T7 (1) and epsilon 15 (24) have previously been reported, this method works only when a clear asymmetric density is seen along one of the icosahedral axes. A resolution of 24 Å for the FAb-33-bound structure is not inconsistent with structures displaying a high degree of noise probably induced by the heterogeneity introduced into the structure by the bound FAb and the variability produced by the induced conformational changes (64).

The biochemical data demonstrating the ability of FAb-33 to promote SVHR sensitivity to proteolysis and to inhibit the fusogenic conformation, together with the virus reconstructions, have led to the development of one model for the neutralization of SVHR by this Ab. This model postulates that a small number of E1 epitopes are bound by FAb-33 molecules and, at some critical occupancy, the virus particle undergoes conformational changes involving the membrane glycoproteins which are subsequently propagated throughout the virus as cascading topological changes. Because virus neutralization occurs rapidly at room temperature, most of the structural changes are probably induced early and quickly. The neutralization curves produced by both Sin-33 and FAb-33 after overnight incubations at 4°C suggest the accumulation of virions in the conformationally neutralized state with time. These Ab-induced conformational changes produce a virus structure which is noninfectious. Sin-33 has previously been reported not to bind to virus boiled in SDS and β-mercaptoethanol (indicating that this Ab did not bind nonspecifically) or to denatured protein. This Ab, however, did bind to virus treated to a pH level of 6.0 (53). As shown herein, after pH 5.3 treatment and a return to a neutral pH, these virions may bind additional Ab or FAb. The increased binding of FAb-33 to virus after low-pH treatment and a return to neutrality suggests that exposure to a low pH makes more Ab binding sites accessible, again indicating that all E1 epitopes were not bound. The resulting neutralized virus structure appears to be "locked" in a dead-end conformation, as shown by the observation that the conformational changes induced by transient exposure to pH 5.3 required for virus-cell fusion do not occur (40). Thus, while the FAb-33 structure can be induced to assume a conformation which can bind additional Ab, the resulting structure remains nonnative. The similarities between Sin-33 and FAb-33 in their abilities to neutralize and bind to virus after exposure to a low

pH suggest that size factors that would place steric constraints on the intact antibody do not play a large role in binding to the E1 epitope.

These data indicate that the neutralization of SVHR by FAb-33 or Sin-33 may occur through a mechanism that exploits the metastable nature of the virus E1 glycoprotein (6, 34, 35) to produce a conformationally neutralized state. FAb-33 binding to SVHR does not induce the major conformational changes seen in reconstructions of low-pH-treated virus, a treatment which also inactivates the virion (40). The structure produced by antibody binding is apparently of an alternate noninfectious form of the virus particle which does not permit the fusion of the virus membrane with the cell membrane after transient exposure to acid pH. Exposure to acid pH did not result in the release of bound antibody; nor did the resultant conformational changes of FAb-33-neutralized SVHR block the attachment of virus to cells. Rather, additional epitopes were exposed, underscoring the metastable nature of the virus particle. We propose that SVHR inactivation in vitro by FAb-33 or Sin-33 is mediated by the induction of a noninfectious conformational intermediate. This metastable structure interferes with the formation of structural rearrangements that are required after binding of the virus to the cell receptor and initiation of the infection. Structural rearrangements of SVHR have previously been shown to occur in response to interactions with the host cell surface (4, 14, 33, 40, 60), most likely upon interaction with the receptor or coreceptor. This proposed mechanism of SVHR neutralization by FAb-33 and Sin-33 is a specific demonstration of a mechanism of virus inactivation which does not require total occlusion of virus epitopes or other forms of steric masking. This is the first reconstruction of an Ab-neutralized enveloped virus showing conformational rearrangements which correlate with the loss of infectivity. This general mechanism of virus neutralization may exist for other metastable enveloped or nonenveloped viruses.

ACKNOWLEDGMENTS

We thank Alan Schmaljohn (U.S. Army Medical Research Institute of Infectious Diseases) for the generous gift of the Sin-33 Ab. Thanks to Michelle West for her excellent technical help. We give special thanks to Wah Chiu for his support and Steve Ludtke for help with EMAN (National Center for Macromolecular Imaging, Verna and Marrs McLean Department of Biochemistry and Molecular Biology, Baylor College of Medicine). Molecular graphics images were produced using the UCSF Chimera package from the Resource for Biocomputing, Visualization, and Informatics at the University of California, San Francisco (see http://www.cgl.ucsf.edu/chimera) (supported by NIH P41 RR-01081).

The cryo-EM work and A.P. were supported by NIH P41RR02250 awarded to Wah Chiu. This research was supported by a grant from the Foundation for Research, Carson City, NV, and by the North Carolina Agricultural Research Service.

REFERENCES

1. **Agirrezabala, X., J. Martin-Benito, J. R. Caston, R. Miranda, J. M. Valpuesta, and J. L. Carrascosa.** 2005. Maturation of phage T7 involves structural modification of both shell and inner core components. EMBO J. **24:**3820–3829.
2. **Anthony, R. P., and D. T. Brown.** 1991. Protein-protein interactions in an Alphavirus membrane. J. Virol. **65:**1187–1194.
3. **Anthony, R. P., A. M. Paredes, and D. T. Brown.** 1992. Disulfide bonds are essential for the stability of the Sindbis virus envelope. Virology **190:**330–336.
4. **Brown, D. T., and J. Edwards.** 1992. Structural changes in Alphaviruses accompanying the process of membrane penetration. Semin. Virol. **3:**519–527.
5. **Cardoso, R. M., M. B. Zwick, R. L. Stanfield, R. Kunert, J. M. Binley, H. Katinger, D. R. Burton, and I. A. Wilson.** 2005. Broadly neutralizing anti-HIV antibody 4E10 recognizes a helical conformation of a highly conserved fusion-associated motif in gp41. Immunity **22:**163–173.
6. **Carleton, M., H. Lee, M. Mulvey, and D. T. Brown.** 1997. Role of glycoprotein PE2 in formation and maturation of the Sindbis virus spike. J. Virol. **71:**1558–1566.
7. **Chang, J., P. Weigele, J. King, W. Chiu, and W. Jiang.** 2006. Cryo-EM asymmetric reconstruction of bacteriophage P22 reveals organization of its DNA packaging and infecting machinery. Structure **14:**1073–1082.
8. **Crowe, J. E., Jr., R. O. Suara, S. Brock, N. Kallewaard, F. House, and J. H. Weitkamp.** 2001. Genetic and structural determinants of virus neutralizing antibodies. Immunol. Res. **23:**135–145.
9. **Eckert, D. M., and P. S. Kim.** 2001. Mechanisms of viral membrane fusion and its inhibition. Annu. Rev. Biochem. **70:**777–810.
10. **Edwards, J., and D. T. Brown.** 1986. Sindbis virus-mediated cell fusion from without is a two-step event. J. Gen. Virol. **67:**377–380.
11. **Edwards, J., E. Mann, and D. T. Brown.** 1983. Conformational changes in Sindbis virus envelope proteins accompanying exposure to low pH. J. Virol. **45:**1090–1097.
12. **Edwards, M. J., and N. J. Dimmock.** 2001. A haemagglutinin (HA1)-specific FAb neutralizes influenza A virus by inhibiting fusion activity. J. Gen. Virol. **82:**1387–1395.
13. **Edwards, M. J., and N. J. Dimmock.** 2001. Hemagglutinin 1-specific immunoglobulin G and Fab molecules mediate postattachment neutralization of influenza A virus by inhibition of an early fusion event. J. Virol. **75:**10208–10218.
14. **Flynn, D. C., W. J. Meyer, J. M. Mackenzie, Jr., and R. E. Johnston.** 1990. A conformational change in Sindbis virus glycoproteins E1 and E2 is detected at the plasma membrane as a consequence of early virus-cell interaction. J. Virol. **64:**3643–3653.
15. **Fuller, S. D.** 1987. The T=4 envelope of Sindbis virus is organized by interactions with a complementary T=3 capsid. Cell **48:**923–934.
16. **Gliedman, J. B., J. F. Smith, and D. T. Brown.** 1975. Morphogenesis of Sindbis virus in cultured *Aedes albopictus* cells. J. Virol. **16:**913–926.
17. **Haag, L., H. Garoff, L. Xing, L. Hammar, S. T. Kan, and R. H. Cheng.** 2002. Acid-induced movements in the glycoprotein shell of an Alphavirus turn the spikes into membrane fusion mode. EMBO J. **21:**4402–4410.
18. **Hernandez, R., D. Ferreira, C. Sinodis, K. Litton, and D. T. Brown.** 2005. Single amino acid insertions at the junction of the Sindbis virus E2 transmembrane domain and endodomain disrupt virus envelopment and alter infectivity. J. Virol. **79:**7682–7697.
19. **Hernandez, R., C. Sinodis, M. Horton, D. Ferreira, C. Yang, and D. T. Brown.** 2003. Deletions in the transmembrane domain of a Sindbis virus glycoprotein alter virus infectivity, stability, and host range. J. Virol. **77:**12710–12719.
20. **Hernandez, R., C. Sinodis, and D. T. Brown.** 2006. Sindbis virus: propagation, quantification and storage, p. 15B.1.2–15B.1.31. *In* R. Coico (ed.), Current protocols in microbiology, unit 15B.1, vol. 1. John Wiley and Sons, Hoboken, NJ.
21. **Imai, M., K. Sugimoto, K. Okazaki, and H. Kida.** 1998. Fusion of influenza virus with the endosomal membrane is inhibited by monoclonal antibodies to defined epitopes on the hemagglutinin. Virus Res. **53:**129–139.
22. **Irie, T., and A. Kawai.** 2005. Further studies on the mechanism of rabies virus neutralization by a viral glycoprotein-specific monoclonal antibody, #1-46-12. Microbiol. Immunol. **49:**721–731.
23. **Irie, T., and A. Kawai.** 2002. Studies on the different conditions for rabies virus neutralization by monoclonal antibodies #1-46-12 and #7-1-9. J. Gen. Virol. **83:**3045–3053.
24. **Jiang, W., J. Chang, J. Jakana, P. Weigele, J. King, and W. Chiu.** 2006. Structure of epsilon15 bacteriophage reveals genome organization and DNA packaging/injection apparatus. Nature **439:**612–616.
25. **Klasse, P. J., and Q. J. Sattentau.** 2002. Occupancy and mechanism in antibody-mediated neutralization of animal viruses. J. Gen. Virol. **83:**2091–2108.
26. **Klimstra, W. B., K. D. Ryman, and R. E. Johnston.** 1998. Adaptation of Sindbis virus to BHK cells selects for use of heparan sulfate as an attachment receptor. J. Virol. **72:**7357–7366.
27. **Kwong, P. D., M. L. Doyle, D. J. Casper, C. Cicala, S. A. Leavitt, S. Majeed, T. D. Steenbeke, M. Venturi, I. Chaiken, M. Fung, H. Katinger, P. W. Parren, J. Robinson, D. Van Ryk, L. Wang, D. R. Burton, E. Freire, R. Wyatt, J. Sodroski, W. A. Hendrickson, and J. Arthos.** 2002. HIV-1 evades antibody-mediated neutralization through conformational masking of receptor-binding sites. Nature **420:**678–682.
28. **Liu, L. N., H. Lee, R. Hernandez, and D. T. Brown.** 1996. Mutations in the endo domain of Sindbis virus glycoprotein E2 block phosphorylation, reorientation of the endo domain, and nucleocapsid binding. Virology **222:**236–246.
29. **Ludtke, S. J., P. R. Baldwin, and W. Chiu.** 1999. EMAN: semiautomated software for high-resolution single-particle reconstructions. J. Struct. Biol. **128:**82–97.
30. **Luo, T., and D. T. Brown.** 1993. Purification and characterization of a Sindbis

virus-induced peptide which stimulates its own production and blocks virus RNA synthesis. Virology **194:**44–49.
31. **Mann, E., J. Edwards, and D. T. Brown.** 1983. Polycaryocyte formation mediated by Sindbis virus glycoproteins. J. Virol. **45:**1083–1089.
32. **McLain, L., and N. J. Dimmock.** 1994. Single- and multi-hit kinetics of immunoglobulin G neutralization of human immunodeficiency virus type 1 by monoclonal antibodies. J. Gen. Virol. **75:**1457–1460.
33. **Meyer, W. J., and R. E. Johnston.** 1993. Structural rearrangement of infecting Sindbis virions at the cell surface: mapping of newly accessible epitopes. J. Virol. **67:**5117–5125.
34. **Mulvey, M., and D. T. Brown.** 1996. Assembly of the Sindbis virus spike protein complex. Virology **219:**125–132.
35. **Mulvey, M., and D. T. Brown.** 1994. Formation and rearrangement of disulfide bonds during maturation of the Sindbis virus E1 glycoprotein. J. Virol. **68:**805–812.
36. **Mulvey, M., and D. T. Brown.** 1995. Involvement of the molecular chaperone BiP in maturation of Sindbis virus envelope glycoproteins. J. Virol. **69:**1621–1627.
37. **Nelson, S., R. Hernandez, D. Ferreira, and D. T. Brown.** 2005. In vivo processing and isolation of furin protease-sensitive Alphavirus glycoproteins: a new technique for producing mutations in virus assembly. Virology **332:**629–639.
38. **Paredes, A., K. Alwell-Warda, S. C. Weaver, W. Chiu, and S. J. Watowich.** 2003. Structure of isolated nucleocapsids from Venezuelan equine encephalitis virus and implications for assembly and disassembly of enveloped virus. J. Virol. **77:**659–664.
39. **Paredes, A. M., D. T. Brown, R. Rothnagel, W. Chiu, R. J. Schoepp, R. E. Johnston, and B. V. Prasad.** 1993. Three-dimensional structure of a membrane-containing virus. Proc. Natl. Acad. Sci. USA **90:**9095–9099.
40. **Paredes, A. M., D. Ferreira, M. Horton, A. Saad, H. Tsuruta, R. Johnston, W. Klimstra, K. Ryman, R. Hernandez, W. Chiu, and D. T. Brown.** 2004. Conformational changes in Sindbis virions resulting from exposure to low pH and interactions with cells suggest that cell penetration may occur at the cell surface in the absence of membrane fusion. Virology **324:**373–386.
41. **Pesavento, J. B., S. E. Crawford, E. Roberts, M. K. Estes, and B. V. Prasad.** 2005. pH-induced conformational change of the rotavirus VP4 spike: implications for cell entry and antibody neutralization. J. Virol. **79:**8572–8580.
42. **Pettersen, E. F., T. D. Goddard, C. C. Huang, G. S. Couch, D. M. Greenblatt, E. C. Meng, and T. E. Ferrin.** 2004. UCSF chimera—a visualization system for exploratory research and analysis. J. Comput. Chem. **25:**1605–1612.
43. **Phinney, B. S., K. Blackburn, and D. T. Brown.** 2000. The surface conformation of Sindbis virus glycoproteins E1 and E2 at neutral and low pH, as determined by mass spectrometry-based mapping. J. Virol. **74:**5667–5678.
44. **Phinney, B. S., and D. T. Brown.** 2000. Sindbis virus glycoprotein E1 is divided into two discrete domains at amino acid 129 by disulfide bridge connections. J. Virol. **74:**9313–9316.
45. **Reading, S. A., and N. J. Dimmock.** 2007. Neutralization of animal virus infectivity by antibody. Arch. Virol. **152:**1047–1059.
46. **Renz, D., and D. T. Brown.** 1976. Characteristics of Sindbis virus temperature-sensitive mutants in cultured BHK-21 and *Aedes albopictus* (mosquito) cells. J. Virol. **19:**775–781.
47. **Roehrig, J. T., A. R. Hunt, R. M. Kinney, and J. H. Mathews.** 1988. In vitro mechanisms of monoclonal antibody neutralization of Alphaviruses. Virology **165:**66–73.
48. **Saad, A., S. J. Ludtke, J. Jakana, F. J. Rixon, H. Tsuruta, and W. Chiu.** 2001. Fourier amplitude decay of electron cryomicroscopic images of single particles and effects on structure determination. J. Struct. Biol. **133:**32–42.
49. **Saad, A., Z. H. Zhou, J. Jakana, W. Chiu, and F. J. Rixon.** 1999. Roles of triplex and scaffolding proteins in herpes simplex virus type 1 capsid formation suggested by structures of recombinant particles. J. Virol. **73:**6821–6830.
50. **Scheefers, H., U. Scheefers-Borchel, J. Edwards, and D. T. Brown.** 1980. Distribution of virus structural proteins and protein-protein interactions in plasma membrane of baby hamster kidney cells infected with Sindbis or vesicular stomatitis virus. Proc. Natl. Acad. Sci. USA **77:**7277–7281.
51. **Scheefers-Borchel, U., H. Scheefers, J. Edwards, and D. T. Brown.** 1981. Sindbis virus maturation in cultured mosquito cells is sensitive to actinomycin D. Virology **110:**292–301.
52. **Schmaljohn, A. L., E. D. Johnson, J. M. Dalrymple, and G. A. Cole.** 1982. Non-neutralizing monoclonal antibodies can prevent lethal Alphavirus encephalitis. Nature **297:**70–72.
53. **Schmaljohn, A. L., K. M. Kokubun, and G. A. Cole.** 1983. Protective monoclonal antibodies define maturational and pH-dependent antigenic changes in Sindbis virus E1 glycoprotein. Virology **130:**144–154.
54. **Smith, T. J.** 2001. Antibody interactions with rhinovirus: lessons for mechanisms of neutralization and the role of immunity in viral evolution. Curr. Top. Microbiol. Immunol. **260:**1–28.
55. **Smith, T. J., R. H. Cheng, N. H. Olson, P. Peterson, E. Chase, R. J. Kuhn, and T. S. Baker.** 1995. Putative receptor binding sites on Alphaviruses as visualized by cryoelectron microscopy. Proc. Natl. Acad. Sci. USA **92:**10648–10652.
56. **Stec, D. S., A. Waddell, C. S. Schmaljohn, G. A. Cole, and A. L. Schmaljohn.** 1986. Antibody-selected variation and reversion in Sindbis virus neutralization epitopes. J. Virol. **57:**715–720.
57. **Strauss, E. G., D. S. Stec, A. L. Schmaljohn, and J. H. Strauss.** 1991. Identification of antigenically important domains in the glycoproteins of Sindbis virus by analysis of antibody escape variants. J. Virol. **65:**4654–4664.
58. **Symington, J., A. K. McCann, and M. J. Schlesinger.** 1977. Infectious virus-antibody complexes of Sindbis virus. Infect. Immun. **15:**720–725.
59. **Tamm, L. K.** 2003. Hypothesis: spring-loaded boomerang mechanism of influenza hemagglutinin-mediated membrane fusion. Biochim. Biophys. Acta **1614:**14–23.
60. **Wang, G., R. Hernandez, K. Weninger, and D. T. Brown.** 2007. Infection of cells by Sindbis virus at low temperature. Virology **362:**461–467.
61. **Wetz, K., P. Willingmann, H. Zeichhardt, and K. O. Habermehl.** 1986. Neutralization of poliovirus by polyclonal antibodies requires binding of a single IgG molecule per virion. Arch. Virol. **91:**207–220.
62. **Wien, M. W., D. J. Filman, E. A. Stura, S. Guillot, F. Delpeyroux, R. Crainic, and J. M. Hogle.** 1995. Structure of the complex between the Fab fragment of a neutralizing antibody for type 1 poliovirus and its viral epitope. Nat. Struct. Biol. **2:**232–243.
63. **Zhang, W., P. R. Chipman, J. Corver, P. R. Johnson, Y. Zhang, S. Mukhopadhyay, T. S. Baker, J. H. Strauss, M. G. Rossmann, and R. J. Kuhn.** 2003. Visualization of membrane protein domains by cryo-electron microscopy of dengue virus. Nat. Struct. Biol. **10:**907–912.
64. **Zhang, W., M. Heil, R. J. Kuhn, and T. S. Baker.** 2005. Heparin binding sites on Ross River virus revealed by electron cryo-microscopy. Virology **332:**511–518.
65. **Zhang, W., S. Mukhopadhyay, S. V. Pletnev, T. S. Baker, R. J. Kuhn, and M. G. Rossmann.** 2002. Placement of the structural proteins in Sindbis virus. J. Virol. **76:**11645–11658.